

# SCIENTIFIC REPORTS



OPEN

## Applications and limitations of fitting of the operational model to determine relative efficacies of agonists

Jan Jakubík<sup>1</sup>, Alena Randáková<sup>1</sup>, Vladimír Rudajev<sup>1</sup>, Pavel Zimčík<sup>1</sup>, Esam E. El-Fakahany<sup>2</sup> & Vladimír Doležal<sup>1</sup>

Proper determination of agonist efficacy is essential in the assessment of agonist selectivity and signalling bias. Agonist efficacy is a relative term that is dependent on the system in which it is measured, especially being dependent on receptor expression level. The operational model (OM) of functional receptor agonism is a useful means for the determination of agonist functional efficacy using the maximal response to agonist and ratio of agonist functional potency to its equilibrium dissociation constant ( $K_A$ ) at the active state of the receptor. However, the functional efficacy parameter  $\tau$  is interdependent on two other parameters of OM; agonist's  $K_A$  and the highest response that could be evoked in the system by any stimulus ( $E_{MAX}$ ). Thus, fitting of OM to functional response data is a tricky process. In this work we analyse pitfalls of fitting OM to experimental data and propose a rigorous fitting procedure where  $K_A$  and  $E_{MAX}$  are derived from half-efficient concentration of agonist and apparent maximal responses obtained from a series of functional response curves. Subsequently, OM with fixed  $K_A$  and  $E_{MAX}$  is fitted to functional response data to obtain  $\tau$ . The procedure was verified at  $M_2$  and  $M_4$  muscarinic receptors fused with the  $G_{15}$  G-protein  $\alpha$ -subunit. The procedure, however, is applicable to any receptor-effector system.

The term “efficacy” is linguistically defined as the ability to produce the desired or intended effect. In pharmacological terms, efficacy means the ability of a chemical to produce a functional response in a cell, tissue or organ. Absolute quantification of efficacy is impossible. Thus, efficacy is rather described in relative terms, e.g. an agonist that produces a more robust maximal response than another is considered more efficacious. In this case the latter agent is described as a partial agonist. However, mere comparison of the magnitude of the maximal response maybe misleading. This is because the apparent maximal response to an agonist is not only a function of its efficacy, but is also dependent on the level of expression of the receptor and signalling entities. For example, a partial agonist may produce an apparent maximal response equal to that of a full agonist in a system with high efficiency of coupling of the receptor to intracellular signal transduction pathways. The relationship between agonist concentration and proportion of receptor occupancy is a mere function of agonist affinity for the given receptor. However, a gradual increase in receptor expression results in proportionally higher numbers (rather than relative proportion) of receptor-agonist complexes. A maximum response is eventually attained due to saturation of downstream effector systems. As a consequence, a partial agonist may reach the maximal response as a full agonist in a high receptor expression system. The potency of an agonist is a measure of the concentration required for exerting a certain level of biological activity, e.g. concentration required to produce its half-maximal effect ( $EC_{50}$ ). Using the same argument as above, a smaller fraction of receptors in a high expression system is needed to form the same number of receptor-agonist complexes. Thus, a lower concentration of agonist is required to produce the same response (i.e. increased “apparent” potency) at higher levels of receptor expression. Taken together, both observed maximal response and potency are system-dependent.

A critical step in screening chemical libraries for new selective agonists is the proper determination of agonist activity that is system-independent. The same criterion is also needed to rule out that apparent agonist selectivity

<sup>1</sup>Institute of Physiology CAS, 142 20, Prague, Czech Republic. <sup>2</sup>Department of Experimental and Clinical Pharmacology, University of Minnesota College of Pharmacy, Minneapolis, MN, 55455, USA. Correspondence and requests for materials should be addressed to J.J. (email: [jan.jakubik@fgu.cas.cz](mailto:jan.jakubik@fgu.cas.cz))

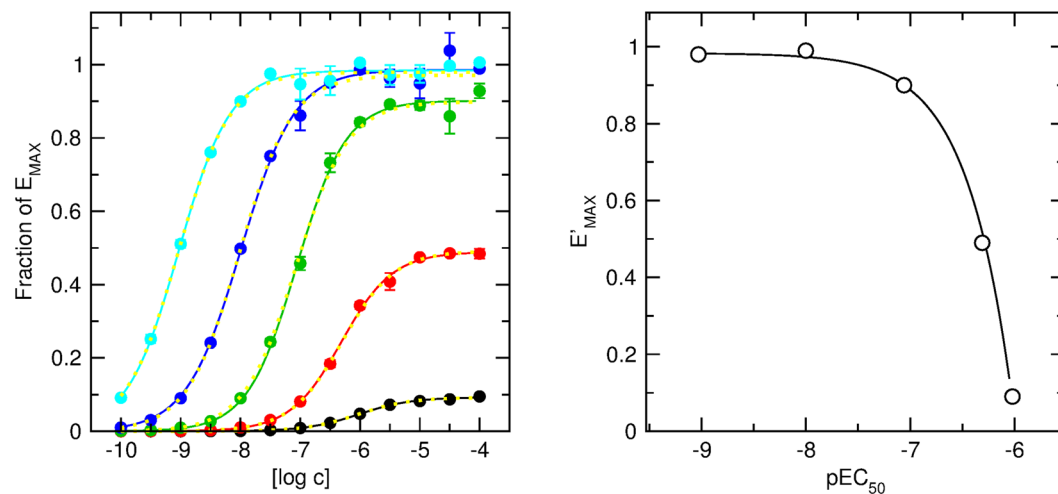


**Figure 1.** Fitting of operational model of agonism (OM) to theoretical concentration-response curves. Left: Simulated data for an agonist with  $\log K_A = -6.0$  in 5 systems with coupling efficacy  $\tau$  varying from 0.1 (black circles) to 1000 (cyan circles). Concentration-response curves were fitted to the simulated data according to Eq. (1). Right: Resulting apparent maximal responses ( $E'_{MAX}$ ) were plotted against resulting half-efficient concentrations ( $EC_{50}$ ). Maximal possible response of the system ( $E_{MAX}$ ) and affinity of agonist for receptor ( $K_A$ ) were obtained by fitting Eq. (6). Calculated  $E_{MAX}$  and  $K_A$  were used in fitting OM Eq. (1) to the data in the left graph (yellow lines). Resulting  $\tau$  are in Table 3.

at a given receptor versus another is an artifact of the test system or assay. Based on these premises the operational model (OM) of pharmacological agonism was formulated<sup>1,2</sup>. This basic OM calculates a parameter  $\tau$  termed “operational efficacy” of agonist from “objective” parameters, namely the equilibrium dissociation constant of agonist ( $K_A$ ) at the active state of the receptor and the maximal response of the system ( $E_{MAX}$ ). OM thus can also rank efficacies of agonists whose responses approach the system  $E_{MAX}$ . Since its formulation, OM has been widely applied in pharmacological analysis in its original form as well as in various modifications and extensions<sup>3,4</sup>.

The major pitfall of application of the OM is that all 3 parameters ( $K_A$ ,  $E_{MAX}$  and  $\tau$ ) are inter-dependent. This constitutes possible difficulties and special requirements in the fitting of the OM to data. We have addressed these issues in the part of our study dedicated to theoretical analysis. We also analysed options to improve robustness of fitting of OM to experimental data. One established way to apply the OM is to determine the value of  $K_A$  experimentally. However, an agonist is not a “mere observer”. Rather, its interaction with the system components affects its affinity<sup>5</sup>. Another established way to fit the OM is to fit at least two dose-response curves sharing some parameters<sup>6</sup>. Finally, we propose a new two-step procedure for the fitting of the OM. We demonstrate benefits of the procedure on the system where, in binding experiments, agonist binding occurs solely to receptors in an inactive conformation, making it impossible to calculate  $K_A$  at the active state of the receptor. We also show that this procedure affords proper ranking of agonist efficacy by fitting of the OM, even when maximal responses to various agonists approach  $E_{MAX}$  of the system. It is impossible to perform direct fitting of OM to data under these conditions using conventional analysis.

## Results

**Evaluation of the theoretical operational model.** The operational model of agonism (OM) is described by following equation:

$$\text{Response} = \frac{[A] * \tau * E_{MAX}}{[A] * (\tau + 1) + K_A} \quad (1)$$

where  $[A]$  is the concentration of an agonist,  $E_{MAX}$  is the maximal response of the system,  $K_A$  is the equilibrium dissociation constant of the agonist-receptor complex and  $\tau$  is the operational factor of efficacy. As can be seen, all 3 parameters ( $E_{MAX}$ ,  $K_A$  and  $\tau$ ) are bound. Clearly, the asymptote of the response curve is given by a product of  $\tau$  and  $E_{MAX}$ . Thus, an increase in  $\tau$  is associated with lowering  $E_{MAX}$  and vice versa. Similarly, the inflection point of the response curve is given by the ratio of  $K_A$  to  $\tau$ ; thus, higher values of  $\tau$  are accompanied by a corresponding increase in  $K_A$ , and vice versa. To evaluate the impact of parameter interdependence on non-linear regression, simulated data of theoretical agonists were generated (see Supplementary information) and the OM was fitted to the simulated data by various procedures. Simulated data of functional response to agonist with 1  $\mu\text{M}$  affinity ( $K_A$ ) were generated by calculation of functional response according to the OM Eq. (1) at 13 concentrations ranging from 0.1 nM to 0.1 mM and addition of 3% of noise (Fig. 1, left). Five sets of simulated data were calculated for 5 values of  $\tau$ , ranging from 0.1 (Fig. 1, black) to 1000 (Fig. 1, cyan) with 10-fold increase in each step. Fitting of the OM to individual datasets resulted in a large error margin of calculated parameters (Table 1). Calculated parameters were correct (close to the simulated ones) only when initial parameter estimates were set to simulated values. When initial parameter estimates were under- or overestimated the calculated parameters were wrong (different

Dataset	$\tau$	$E_{MAX}$	$\log K_A$
<b>Individual fits</b>			
A	0.1017 ± 143155	1.00 ± 1278802	-5.98 ± 56434
B	0.9770 ± 963950	0.99 ± 494776	-6.01 ± 211757
C	10.28 ± 8530181	0.99 ± 73080	-6.00 ± 328416
D	99.43 ± 109608398	0.99 ± 10893	-6.00 ± 473965
E	1074 ± 558660685	0.98 ± 476	-6.00 ± 225560
<b>Global fit with shared <math>E_{MAX}</math></b>			
A	0.1033 ± 0.0297	0.99 ± 0.01	-5.98 ± 0.58
B	0.9872 ± 0.0898	0.99 ± 0.01	-6.01 ± 0.12
C	11.12 ± 3.08	0.99 ± 0.01	-5.97 ± 0.14
D	224 ± 683	0.99 ± 0.01	-5.66 ± 1.32
E	971 ± 3064	0.99 ± 0.01	-6.03 ± 1.37
<b>Global fit with shared <math>E_{MAX}</math> and <math>K_A</math></b>			
A	0.1026 ± 0.0237	0.99 ± 0.01	-5.99 ± 0.09
B	0.9910 ± 0.0847	0.99 ± 0.01	-5.99 ± 0.09
C	10.64 ± 2.01	0.99 ± 0.01	-5.99 ± 0.09
D	102.5 ± 24.2	0.99 ± 0.01	-5.99 ± 0.09
E	1084 ± 259	0.99 ± 0.01	-5.99 ± 0.09

**Table 1.** Fitting OM to simulated data. Simulation parameters  $\log K_A = -6$ ,  $E_{MAX} = 1$ ; curve A,  $\tau = 0.1$ ; curve B,  $\tau = 1$ ; curve C,  $\tau = 10$ ; curve D,  $\tau = 100$ ; curve E,  $\tau = 1000$ . Values are parameter estimates ± SD.

from simulated ones) (Supplementary information, Fig. SI1). Specifically, a low initial estimate of  $E_{MAX}$  resulted in overestimated  $\tau$  and high initial estimate of  $E_{MAX}$  resulted in underestimated  $\tau$  in most cases. This confirms that all 3 parameters of the OM are inter-bound. Under these conditions the error margin is so large that it is impossible to estimate OM parameters from individual fits.

It is a requisite to check the distribution of estimated parameters before proceeding with statistical analysis. In pharmacological calculations, many parameters need to be converted to logarithm to remove skewness. To analyse the distribution of parameter  $\tau$ , 1000 sets of concentration-response curves were simulated. Equation (1) was fitted to these datasets in two forms, one with parameter  $\tau$  and another with parameter  $\log(\tau)$  (Supplementary information, Fig. SI2). In contrast to previous findings<sup>7</sup>, analysis of  $\tau$  and  $\log(\tau)$  distribution has shown that whether to use  $\tau$  or  $\log(\tau)$  in Eq. (1) is irrelevant.

As simulated data are for the same system they share parameter  $E_{MAX}$ . Global fit of all 5 datasets with shared  $E_{MAX}$  reduced fit error (Table 1). The standard deviation of  $E_{MAX}$  fell down to 1%. However, SD of parameter  $\tau$  was still several hundreds of % for datasets D and E. As simulated data are modelled for one agonist,  $K_A$  is a shared parameter of all datasets too. Global fit of all 5 datasets with shared  $E_{MAX}$  and  $K_A$  parameters further reduced fit error, SD of  $E_{MAX}$  remained at 1%, SD of  $K_A$  was 0.09 log unit and SD of operational efficacy  $\tau$  was lowest for dataset B (8.5%) and gradually increased with changes in  $\tau$  value in both directions up to 24%. This confirms previous findings showing the necessity to fit the OM simultaneously to at least two concentration-response curves with shared parameters<sup>6</sup>.

In practice, experimenter may determine agonist affinity for the receptor in a different kind of experiments, e.g. radioligand binding. The impact of fixing  $K_A$  to simulated value is summarized in Table 2. Fixing  $K_A$  to a correct value tremendously reduced fit error. For datasets C, D and E with the highest operational efficacy, SD of  $E_{MAX}$  was 1% and SD of parameter  $\tau$  was about 6%. On the other hand, for dataset A with the lowest efficacy, SD of  $E_{MAX}$  was 54% and SD of parameter  $\tau$  was 68%. According to the OM,  $EC_{50}$  is related to  $K_A$  according to the following equation.

$$EC_{50} = \frac{K_A}{\tau + 1} \quad (2)$$

According to Eq. (2), higher operational efficacy  $\tau$  means lower  $EC_{50}$ , i.e., a greater left-ward shift of  $EC_{50}$  from  $K_A$ . Because the accuracy of determination of  $EC_{50}$  is constant (on a logarithmic scale), the inaccuracy in  $EC_{50}$  determination represents proportionally greater error in low efficacy systems, where the difference between  $EC_{50}$  and  $K_A$  is small. Operational efficacy  $\tau$  is bound to  $E_{MAX}$ . Thus, the proportionally large error in estimation of operational efficacy  $\tau$  is translated to a large error in estimation of  $E_{MAX}$ . Fitting of the OM to all 5 datasets with fixed  $K_A$  and shared  $E_{MAX}$  led to an increase in the  $\tau$  SD for datasets D and E. Although the increase in SDs after reducing the number of fitted parameters may seem counter-intuitive at first glance, it could be explained by the approach of  $E_{MAX}$  to system  $E_{MAX}$ . Moreover, the increase in  $\tau$  SD for datasets D and E is compensated by the reduction of  $\tau$  SD for datasets A and B.

Although fixing  $K_A$  in the model system results in estimates of  $E_{MAX}$  and  $\tau$  that are close to the model values, the fitting procedure is still not robust. This is evidenced by the high SD values of  $E_{MAX}$  and  $\tau$  estimates for dataset A (Table 2). When fitting Eq. (1) with fixed  $K_A$  and shared  $E_{MAX}$ , SD of  $E_{MAX}$  falls to 1% but SD of parameter  $\tau$  remains relatively high. Furthermore, to obtain correct  $K_A$ , the experimenter must replicate the same conditions of functional response assay in the ligand binding assay. This may be technically difficult when functional assay is

Dataset	$\tau$	$E_{MAX}$	$\log K_A$
<b>Individual fits</b>			
A	0.0844 ± 0.0571	1.00 ± 0.54	−6
B	1.025 ± 0.096	0.97 ± 0.05	−6
C	10.32 ± 0.71	0.99 ± 0.01	−6
D	99.43 ± 6.80	0.99 ± 0.01	−6
E	1077 ± 52	0.98 ± 0.01	−6
<b>Global fit with shared <math>E_{MAX}</math></b>			
A	0.1024 ± 0.0223	0.99 ± 0.01	−6
B	0.9869 ± 0.0641	0.99 ± 0.01	−6
C	10.50 ± 0.93	0.99 ± 0.01	−6
D	100.8 ± 9.9	0.99 ± 0.01	−6
E	1065 ± 105	0.99 ± 0.01	−6

**Table 2.** Fitting OM with fixed  $K_A$  to simulated data. Simulation parameters  $\log K_A = -6$ ,  $E_{MAX} = 1$ ; curve A,  $\tau = 0.1$ ; curve B,  $\tau = 1$ ; curve C,  $\tau = 10$ ; curve D,  $\tau = 100$ ; curve E,  $\tau = 1000$ . Values are parameter estimates ± SD.

Dataset	$\tau$	$E_{MAX}$	$\log K_A$
<b>Individual fits</b>			
A	0.1036 ± 0.0009	0.98	−5.99
B	1.008 ± 0.013	0.98	−5.99
C	11.04 ± 0.48	0.98	−5.99
D	106.1 ± 6.7	0.98	−5.99
E	1119 ± 50	0.98	−5.99

**Table 3.** Fitting OM with fixed  $K_A$  and  $E_{MAX}$  to simulated data. Simulation parameters  $\log K_A = -6$ ,  $E_{MAX} = 1$ ; curve A,  $\tau = 0.1$ ; curve B,  $\tau = 1$ ; curve C,  $\tau = 10$ ; curve D,  $\tau = 100$ ; curve E,  $\tau = 1000$ .  $K_A$  and  $E_{MAX}$  were fixed to values obtained from  $E'_{MAX}$  versus  $EC_{50}$  plot (Fig. 1, right). Values are parameter estimates ± SD.

carried out at complicated system that is incompatible with radioligand binding assay. Therefore, we searched for an alternative way to obtain the value of all 3 parameters of the OM without a need to fit equation(s) that contain inter-bound parameters. The apparent maximal response  $E'_{MAX}$  observed as the upper asymptote of the functional response curve is given by the following equation.

$$E'_{MAX} = \frac{E_{MAX} * \tau}{\tau + 1} \quad (3)$$

By rearrangement of Eq. (2),  $\tau$  can be expressed as follows.

$$\tau = \frac{K_A - EC_{50}}{EC_{50}} \quad (4)$$

Substitution of  $\tau$  in Eq. (3) results in:

$$E'_{MAX} = \frac{\frac{E_{MAX} * K_A - EC_{50}}{EC_{50}}}{\frac{K_A - EC_{50}}{EC_{50}} + 1} \quad (5)$$

After rearrangement and simplification of Eq. (5) we get:

$$E'_{MAX} = E_{MAX} - \frac{E_{MAX} * EC_{50}}{K_A} \quad (6)$$

Apparent maximal response  $E'_{MAX}$  and half-efficient concentration  $EC_{50}$  can be reliably obtained by fitting logistic function (Eq. (10), see Methods) to individual concentration-response curves. After plotting  $E'_{MAX}$  versus the corresponding  $EC_{50}$ , fitting Eq. (6) yields a maximal response of the system ( $E_{MAX}$ ) and the equilibrium dissociation constant of the agonist-receptor complex ( $K_A$ ).

Simulated data (Fig. 1, left) were fitted with Eq. (10) and resulting  $E'_{MAX}$  values were plotted against corresponding  $EC_{50}$  values (Fig. 1, right). Fitting Eq. (6) to the data yielded system  $E_{MAX} = 0.98 \pm 0.01$  and logarithm of the equilibrium dissociation constant of the agonist-receptor complex  $K_A = -5.99 \pm 0.01$  (parameter estimate ± SD). Subsequently, the OM of functional response Eq. (1) with  $E_{MAX}$  fixed to 0.98 and  $\log K_A$  fixed to  $-5.99$  was fitted to simulated data (Fig. 1, left, yellow curves). The standard deviation of the operational efficacy

Cell line	$[^3\text{H}]\text{NMS}$		carbachol	oxotremorine	pilocarpine
	$\text{pK}_D$	$B_{\text{MAX}}$	$\text{pK}_I$	$\text{pK}_I$	$\text{pK}_I$
$M_2\_G_{15}$ #1	9.56 ± 0.02	11.4 ± 0.5	4.63 ± 0.02	5.72 ± 0.03	4.49 ± 0.03
$M_2\_G_{15}$ #2	9.56 ± 0.02	5.40 ± 0.09	4.61 ± 0.02	5.76 ± 0.03	4.52 ± 0.02
$M_2\_G_{15}$ #3	9.55 ± 0.02	2.52 ± 0.05	4.64 ± 0.02	5.78 ± 0.03	4.51 ± 0.02
$M_2\_G_{15}$ #4	9.57 ± 0.02	1.82 ± 0.03	4.63 ± 0.02	5.75 ± 0.02	4.54 ± 0.03
$M_2\_G_{15}$ #5	9.55 ± 0.02	0.87 ± 0.01	4.64 ± 0.02	5.73 ± 0.03	4.50 ± 0.02
$M_4\_G_{15}$ #1	9.72 ± 0.02	14.6 ± 0.7	4.63 ± 0.02	5.86 ± 0.03	4.55 ± 0.03
$M_4\_G_{15}$ #2	9.73 ± 0.02	6.02 ± 0.08	4.65 ± 0.02	5.84 ± 0.03	4.54 ± 0.02
$M_4\_G_{15}$ #3	9.72 ± 0.02	2.11 ± 0.06	4.62 ± 0.02	5.83 ± 0.03	4.51 ± 0.03
$M_4\_G_{15}$ #4	9.71 ± 0.02	1.33 ± 0.04	4.63 ± 0.02	5.80 ± 0.03	4.53 ± 0.02
$M_4\_G_{15}$ #5	9.75 ± 0.03	0.53 ± 0.02	4.62 ± 0.02	5.82 ± 0.03	4.52 ± 0.02

**Table 4.** Binding parameters of fusion proteins of muscarinic receptor and  $G_{15}$  G-protein in CHO cell lines. Equilibrium dissociation constant ( $K_D$ ) and maximum binding capacity ( $B_{\text{MAX}}$ ) were obtained by fitting Eq. (7) to the data from  $[^3\text{H}]\text{NMS}$  saturation experiments.  $B_{\text{MAX}}$  is expressed as pmol binding sites per mg of protein. Inhibition constants ( $K_I$ ) were calculated according Eq. (9) from  $\text{IC}_{50}$  values that were obtained by fitting Eq. (8) to the data from competition experiments of agonist and  $[^3\text{H}]\text{NMS}$ . Data are means ± SD from 3 independent experiments performed in quadruplicates.

parameter  $\tau$  ranged from less than 1% for dataset A to 6% for dataset D, that is a substantial improvement over fitting of the OM Eq. (1) with shared  $E_{\text{MAX}}$  and fixed  $K_A$  (Table 3 vs. Table 2).

**Binding experiments.** Five cell lines with various expression levels were chosen from newly established cell lines expressing fusion proteins of muscarinic receptor and the  $G_{15}$  G-protein. The expression level was determined in saturation binding experiments (Table 4). The expression level ranged from 0.87 to 14.6 pmol of binding sites per mg of protein for the  $M_2\_G_{15}$  fusion protein and from 0.53 to 14.6 pmol of binding sites per mg of protein for the  $M_4\_G_{15}$  fusion protein, respectively (Table 4). Expression level was stable among passages. Expression level had no effect on the equilibrium dissociation constant  $K_D$  of N- $[^3\text{H}]\text{methylscopolamine}$  ( $[^3\text{H}]\text{NMS}$ ). Fusion of G-protein to receptor resulted in a slightly lower  $K_D$  (higher affinity) of  $[^3\text{H}]\text{NMS}$  than the wild-type receptor<sup>8</sup>. Inhibition constants  $K_I$  of carbachol, oxotremorine and pilocarpine, respectively, were determined in competition experiments with 1 nM  $[^3\text{H}]\text{NMS}$ . All 3 agonists displayed binding to a single low-affinity site. Expression level had no effect on the equilibrium dissociation constant  $K_I$  of any of the tested agonists (Table 4).

**Functional response to agonists.**  $M_2$  and  $M_4$  receptors were coupled to the phospholipase C pathway by  $G_{15}$  G-protein<sup>9</sup>. The level of inositol phosphates ( $\text{IP}_X$ ) was taken as a measure of functional response. Response to agonists was plotted as folds over basal (Figs 2 and 3). Analysis of the theoretical model of the OM fitting of Eq. (1) to individual response curves resulted in expected large errors in estimation of fitted parameters. Unfortunately, values of inhibition constants ( $K_I$ ) obtained from binding experiments could not be used as  $K_A$  values in the fitting of Eq. (1) to the functional response data (Supplementary Information, Figs SI3–SI8). In fitting individual response curves, fixing  $K_A$  to  $K_I$  value resulted in good fit with high values of  $\tau$  and variation in  $E_{\text{MAX}}$  estimates (Supplementary Information, Figs SI3–SI8, full lines). Fitting response curves with shared  $E_{\text{MAX}}$  resulted in poor fits (Supplementary Information, Figs SI3–SI8, dotted yellow lines). According to Eq. (4), large (100 to 1000-fold) differences between  $K_I$  and half-efficient concentrations ( $\text{EC}_{50}$ ) correspond to large (100 to 1000) values of  $\tau$ . According to Eq. (3), for very large values of  $\tau$  the apparent maximal response  $E'_{\text{MAX}}$  should be very close to the maximal response of the system  $E_{\text{MAX}}$ . Therefore, apparent  $E'_{\text{MAX}}$  should theoretically be the same for all receptor expression levels. Obviously, this is not the case here (Figs 2 and 3).

Therefore, a new fitting procedure was employed in which maximal response of the system ( $E_{\text{MAX}}$ ) and agonist equilibrium dissociation constant ( $K_A$ ) were determined first and then  $E_{\text{MAX}}$  and  $K_A$  values were used in fitting of the OM to the functional response data. Specifically, Eq. (10) was fitted to the data and apparent maximal response ( $E'_{\text{MAX}}$ ), half-efficient concentration ( $\text{EC}_{50}$ ) and slope factor (nH) were determined. All concentration-response curves displayed nH equal to unity. Expression level affected both  $E'_{\text{MAX}}$  and  $\text{EC}_{50}$ . Increase in expression level resulted in an increase in  $E'_{\text{MAX}}$  and a decrease in  $\text{EC}_{50}$ . The magnitude of effects of expression level on functional response at  $M_2\_G_{15}$  was similar to that at  $M_4\_G_{15}$ . Calculated  $E'_{\text{MAX}}$  values were plotted against corresponding  $\text{EC}_{50}$  values (Figs 2 and 3, right bottom plots) and Eq. (6) was fitted to the data. Fitting of Eq. (6) to experimental data resulted in the same  $E_{\text{MAX}}$  for all 3 agonists confirming that the cell clones had the same  $E_{\text{MAX}}$ . Resulting  $E_{\text{MAX}}$  and  $K_A$  values were used in the subsequent fitting of Eq. (1) to the functional response data (after subtraction of basal level). For a given agonist global fit of Eq. (1) was performed in all 5 cell lines (Figs 2 and 3, yellow lines). Calculated values of the operational efficacy factor ( $\tau$ ) are summarized in Tables 5 and 6.

Basal activity of  $M_2$  and  $M_4$  fusion proteins was  $16 \pm 1$  and  $21 \pm 1\%$  of incorporated radioactivity (mean ± SD,  $n = 3$ ), respectively (Figs 2 and 3).  $E_{\text{MAX}}$  estimated according to Eq. (6) ranged from 91 to 93% of incorporated radioactivity at  $M_2$  and from 85 to 89% of incorporated radioactivity at  $M_4$  fusion protein.

Subsequently, functional responses to 9 muscarinic agonists in cell clones with medium expression of fusion protein ( $M_2\_G_{15}\#3$  and  $M_4\_G_{15}\#3$ ) was measured in three ways: As stimulation of  $[^3\text{S}]\text{GTP}\gamma\text{S}$  binding, as accumulation of  $\text{IP}_X$ , and as changes in the level of intracellular calcium (Figs 4 and 5; Tables 7 and 8). Muscarinic agonists included classical full and partial agonists, the superagonist iperexo, the bitopic agonist McN-A-343 and

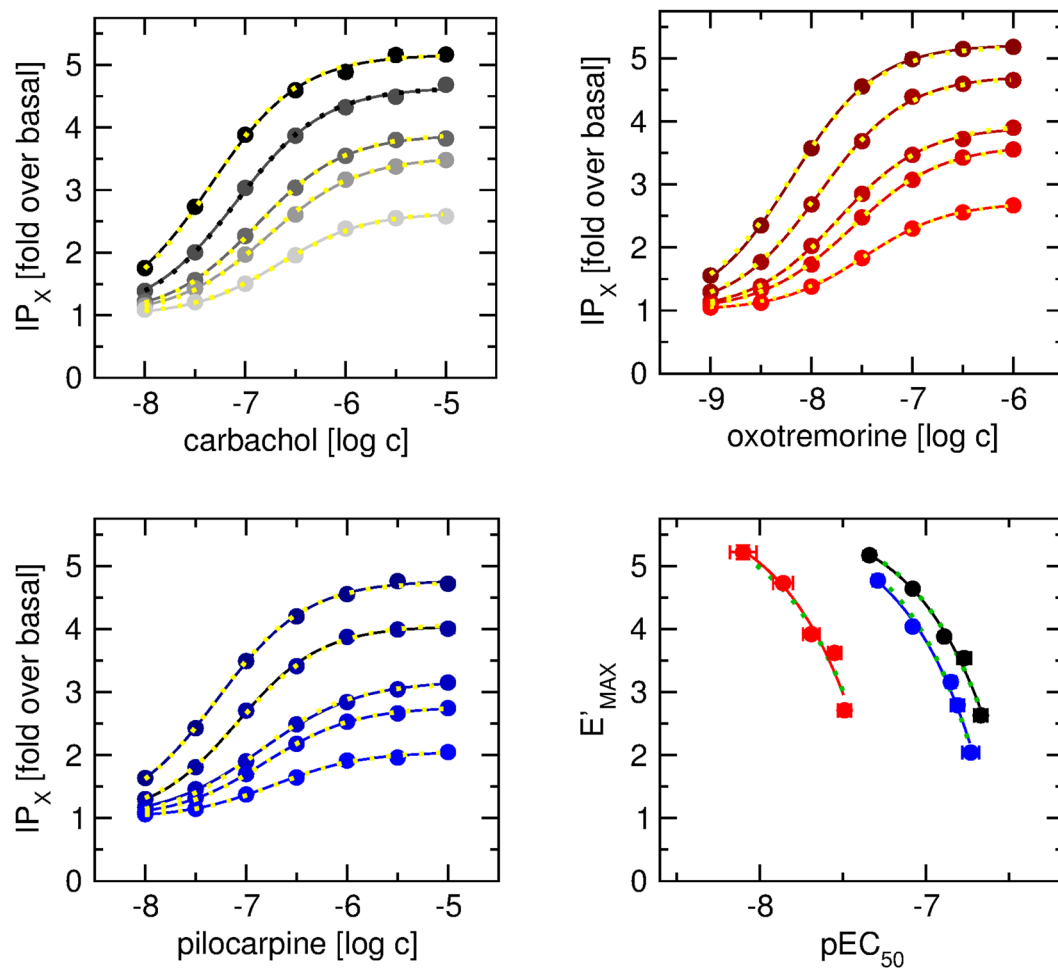


**Figure 2.** Fitting of the OM to concentration response curves in cells expressing  $M_2$ - $G_{15}$  fusion protein. Level of inositol phosphates ( $IP_x$ ) was taken as the functional response measure and is expressed as folds over basal level ( $16 \pm 1\%$  of incorporated radioactivity). Eq. (10) was fitted to data of functional response (solid lines) to carbachol (upper left), oxotremorine (upper right) and pilocarpine (lower left) at cells expressing  $M_2$ - $G_{15}$  fusion protein at various levels. After subtraction of basal value Eq. (6) was fitted to  $E'_{MAX}$  versus  $EC_{50}$  plot (lower right) of functional response to carbachol (black), oxotremorine (red) and pilocarpine (blue) to obtain  $E_{MAX}$  and  $K_A$  values, solid lines – individual fits, green dotted lines – shared  $E_{MAX}$  fit. Eq. (1) with fixed  $E_{MAX}$  and  $K_A$  parameters was fitted to data of functional response (dotted yellow lines). Data are means  $\pm$  SD from 3 independent experiments performed in quadruplicates.

the atypical agonists N-desmethylclozapine and xanomeline. First, Eq. (10) was fitted to individual data sets. After subtraction of basal value, Eq. (6) was fitted to  $E'_{MAX}$  versus  $EC_{50}$  data from all 3 experiments for all agonists to obtain  $E_{MAX}$  of the assay. Then Eq. (1) with fixed  $E_{MAX}$  was fitted to individual functional responses. In  $IP_x$  assay,  $\tau$  values of the agonists carbachol, oxotremorine and pilocarpine were the same as in simultaneous fitting of OM to all five clones where both  $K_A$  and  $E_{MAX}$  were fixed (Figs 2 and 3; Tables 5 and 6). However, estimates of parameter  $\tau$  were accompanied by greater SD. In  $[^{35}S]GTP\gamma S$  binding and  $IP_x$  assays the functional response even to the superagonist iperoxo was less than 90% at  $M_2$ - $G_{15}$  and less than 80% at  $M_4$ - $G_{15}$ . In these assays relative SD of  $\tau$  was about 10%. In intracellular  $Ca^{2+}$  mobilisation assay the functional response to iperoxo reached 99% of  $E_{MAX}$ . In this assay relative SD of  $\tau$  ranged from 15 to 34%, being much lower than that in case of direct fitting of OM with shared  $E_{MAX}$ . In intracellular  $Ca^{2+}$  mobilisation assay, agonist ranking by parameter  $\tau$  was the same as in  $[^{35}S]GTP\gamma S$  and  $IP_x$  assays. Also, the estimates of  $K_A$  were the same in all assays.

## Discussion

Proper determination of agonist efficacy is a cornerstone in the assessment of possible agonist selectivity and signalling bias. Agonist efficacy at a given receptor or receptor subtype is affected by the system in which it is determined. Black and Leff<sup>1</sup> presented a model, termed the operational model of agonism (OM) of receptor-effector systems. In its original principle, the OM is applicable to any receptor effector system. Over time the OM became a golden standard in pharmacological analysis<sup>3,4</sup>. Extended and modified versions of this model are widely applied, not only to agonist action, but also to allosteric activation and allosteric modulation<sup>10–14</sup> or to analyse agonist signalling bias at GPCRs<sup>15–18</sup> as well as non-GPCRs<sup>19</sup>.

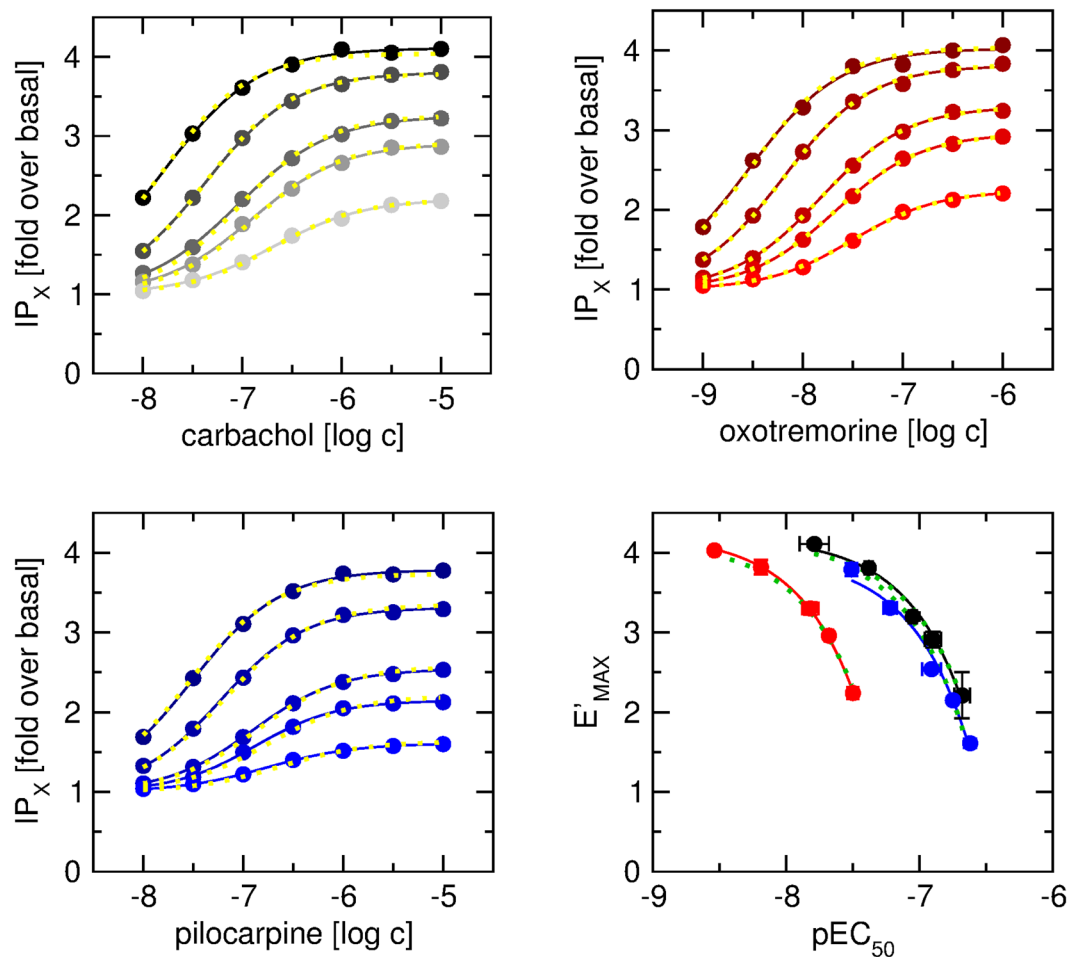


**Figure 3.** Fitting of the OM to concentration response curves in cells expressing M<sub>4</sub>-G<sub>15</sub> fusion protein. Level of inositol phosphates (IP<sub>x</sub>) was taken as functional response measure and is expressed as folds over basal level (21 ± 1% of incorporated radioactivity). Eq. (10) was fitted to data of functional response (solid lines) to carbachol (upper left), oxotremorine (upper right) and pilocarpine (lower left) at cells expressing M<sub>2</sub>-G<sub>15</sub> fusion protein at various levels. After subtraction of basal value Eq. (6) was fitted to E' MAX versus EC<sub>50</sub> plot (lower right) of functional response to carbachol (black), oxotremorine (red) and pilocarpine (blue) to obtain E' MAX and K<sub>A</sub> values, solid lines – individual fits, green dotted lines – shared E' MAX fit. Eq. (1) with fixed E' MAX and K<sub>A</sub> parameters was fitted to data of functional response (dotted yellow lines). Data are means ± SD from 3 independent experiments performed in quadruplicates.

	carbachol	oxotremorine	pilocarpine
E' MAX	5.81 ± 0.12	5.77 ± 0.14	5.68 ± 0.10
pK <sub>A</sub>	6.47 ± 0.04	7.28 ± 0.03	6.60 ± 0.02
τ			
M <sub>2</sub> -G <sub>15</sub> #1	6.75 ± 0.20	6.93 ± 0.21	1.73 ± 0.03
M <sub>2</sub> -G <sub>15</sub> #2	3.22 ± 0.18	3.43 ± 0.09	1.44 ± 0.01
M <sub>2</sub> -G <sub>15</sub> #3	1.50 ± 0.04	2.59 ± 0.04	0.781 ± 0.011
M <sub>2</sub> -G <sub>15</sub> #4	1.08 ± 0.02	1.47 ± 0.02	0.555 ± 0.005
M <sub>2</sub> -G <sub>15</sub> #5	0.521 ± 0.008	0.578 ± 0.008	0.199 ± 0.006

**Table 5.** Parameters of functional response of fusion protein of M<sub>2</sub> muscarinic receptor and G<sub>15</sub> G-protein in CHO cell lines. Maximal response of the system (E' MAX) and equilibrium dissociation constant of the agonist-receptor complex (K<sub>A</sub>) were calculated by fitting Eq. (6) to E' MAX versus EC<sub>50</sub> plot in Fig. 2. The operational factor of efficacy (τ) was obtained by fitting Eq. (1) with fixed E' MAX and K<sub>A</sub> to concentration response curves in Fig. 2. Data are means ± SD from 3 independent experiments performed in quadruplicates.

	carbachol	oxotremorine	pilocarpine
$E_{MAX}$	$4.19 \pm 0.08$	$4.22 \pm 0.02$	$4.03 \pm 0.14$
$pK_A$	$6.48 \pm 0.04$	$7.28 \pm 0.02$	$6.53 \pm 0.01$
$\tau$			
$M_4\_G_{15}$ #1	$15.7 \pm 0.4$	$17.0 \pm 0.5$	$9.41 \pm 0.50$
$M_4\_G_{15}$ #2	$7.02 \pm 0.38$	$7.54 \pm 0.34$	$3.48 \pm 0.15$
$M_4\_G_{15}$ #3	$2.46 \pm 0.25$	$2.49 \pm 0.08$	$1.08 \pm 0.02$
$M_4\_G_{15}$ #4	$1.55 \pm 0.12$	$1.64 \pm 0.04$	$0.66 \pm 0.01$
$M_4\_G_{15}$ #5	$0.720 \pm 0.097$	$0.835 \pm 0.015$	$0.265 \pm 0.013$

**Table 6.** Parameters of functional response of fusion protein of  $M_4$  muscarinic receptor and  $G_{15}$  G-protein in CHO cell lines. Maximal response of the system ( $E_{MAX}$ ) and equilibrium dissociation constant of the agonist-receptor complex ( $K_A$ ) were calculated by fitting Eq. (6) to  $E'_{MAX}$  versus  $EC_{50}$  plot in Fig. 3. The operational factor of efficacy ( $\tau$ ) was obtained by fitting Eq. (1) with fixed parameters  $E_{MAX}$  and  $K_A$  to concentration response curves in Fig. 3. Data are means  $\pm$  SD from 3 independent experiments performed in quadruplicates.

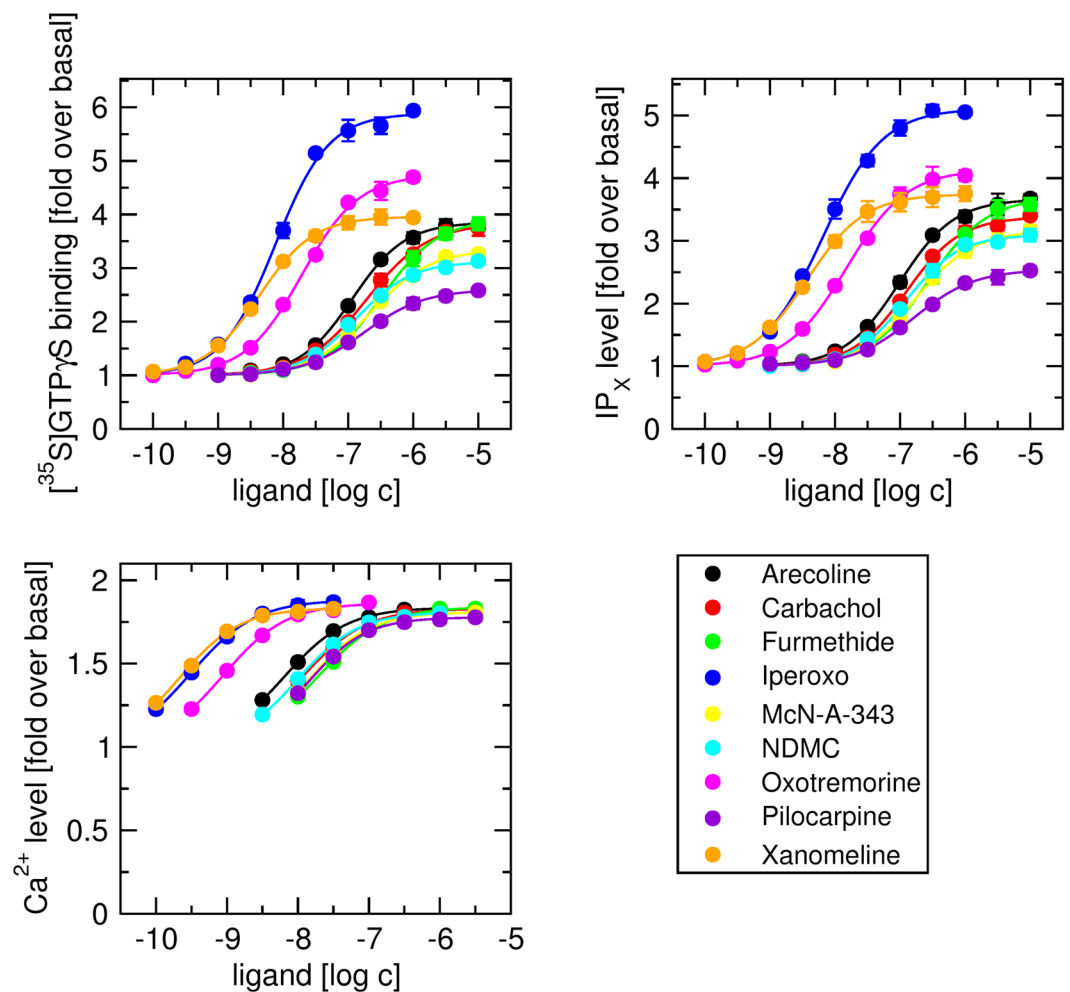


**Figure 4.** Functional response of cells expressing  $M_2\_G_{15}$  fusion protein to muscarinic agonists. Level of  $[^{35}S]$  GTP $\gamma$ S binding (upper left), inositol phosphates ( $IP_x$ ) (upper right) and intracellular calcium (lower left) was taken as functional response to muscarinic agonists (indicated in legend) of cells expressing  $M_2\_G_{15}$  fusion protein and is expressed as folds over basal level. Eq. (10) was fitted to individual data sets. After subtraction of basal value Eq. (6) was fitted to  $E'_{MAX}$  versus  $EC_{50}$  data from all 3 experiments for all agonists to obtain  $E_{MAX}$  of the assay. Eq. (1) with fixed  $E_{MAX}$  was fitted to individual functional responses. Results are summarized in Table 7. Data are means  $\pm$  SD from 3 independent experiments.

In the present work we explored potential pitfalls of application of the original OM to fit experimental data. We present a simple procedure for reliable fitting of the OM to experimental data. The procedure divides actual fitting of OM to two steps. Individual steps have lower number of degrees of freedom and thus result in more



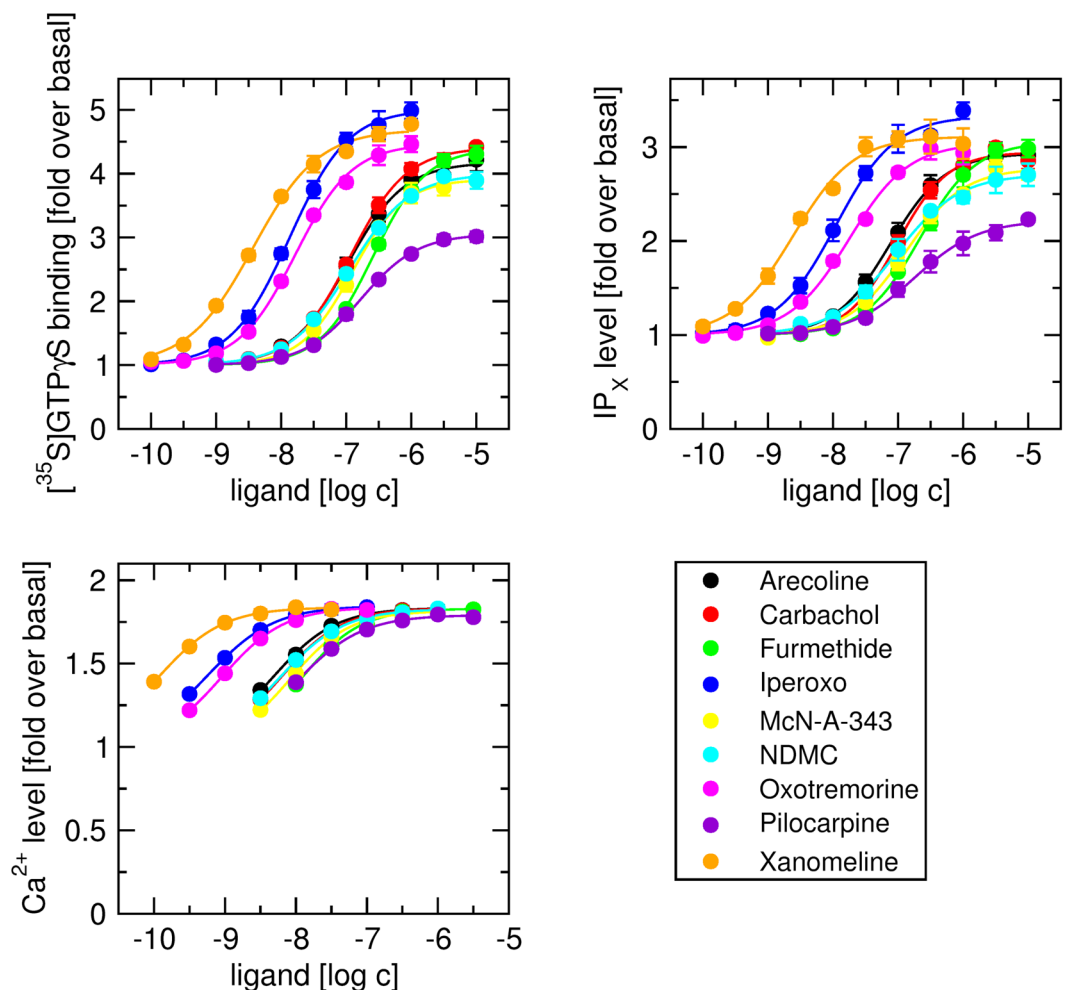


**Figure 5.** Functional response of cells expressing  $M_4\_G_{15}$  fusion protein to muscarinic agonists. Level of  $[^{35}\text{S}]\text{GTP}\gamma\text{S}$  binding (upper left), inositol phosphates ( $\text{IP}_x$ ) (upper right) and intracellular calcium (lower left) was taken as functional response to muscarinic agonists (indicated in legend) of cells expressing  $M_4\_G_{15}$  fusion protein and is expressed as folds over basal level. Eq. (10) was fitted to individual data sets. After subtraction of basal value Eq. (6) was fitted to  $E_{\text{MAX}}$  versus  $\text{EC}_{50}$  data from all 3 experiments for all agonists to obtain  $E_{\text{MAX}}$  of the assay. Eq. (1) with fixed  $E_{\text{MAX}}$  was fitted to individual functional responses. Results are summarized in Table 8. Data are means  $\pm$  SD from 3 independent experiments.

reliable parameter estimates. We demonstrate usefulness of this procedure in a system where the affinity of the agonist for the receptor in active state cannot be reliably determined in binding experiments and also in a system where the functional response to the agonist approaches the maximal response of the system.

Response to an agonist is affected by the system, mainly by the expression level of the receptor. Mass action law dictates that the relationship between occupancy and effect must be hyperbolic. Therefore, response to agonist according to the OM is described by Eq. (1), where  $E_{\text{MAX}}$  is the maximal response of the system,  $K_A$  is the agonist equilibrium dissociation constant at the receptor in an active conformation and  $\tau$  is the operational efficacy<sup>1</sup>. All 3 parameters ( $E_{\text{MAX}}$ ,  $K_A$  and  $\tau$ ) of Eq. (1) are inter-bound and thus Eq. (1) should be fitted to at least two concentration-response curves with shared parameters<sup>6</sup>. The asymptote of the response curve is given by the product of  $\tau$  and  $E_{\text{MAX}}$  and inflection point is given by the ratio of  $K_A$  to  $\tau$ . Thus,  $K_A$  is also inter-bound to  $E_{\text{MAX}}$  via  $\tau$ . Functions with inter-bound parameters generally have flat curvature of sum of error function that prevents finding its global minimum and estimation of fitted parameters is therefore associated with large error margins. This was confirmed by fitting of Eq. (1) to individual response curves of the theoretical model system (Fig. 1, Tables 1 and 2). Moreover, result of fit (parameter estimates) is influenced by initial values of fitted parameters (Supplementary Information, Fig. S11). Further analysis of the theoretical model system showed that major improvement of fit is achieved by fixing  $K_A$  value while performing global fit with shared  $E_{\text{MAX}}$ . Thus, precise determination of  $K_A$  turns to be corner stone in application of the OM. However, in contrast to previous findings<sup>7</sup>, analysis of parameter  $\tau$  distribution was independent of whether  $\tau$  or  $\log(\tau)$  is used (Supplementary information, Fig. S12).

Experimental conditions (like temperature, ionic strength, solution composition, receptor environment) affect agonist  $K_A$ . Thus, when  $K_A$  is determined in different kinds of experiment (e.g. radioligand binding assay), conditions of the assay have to strictly mimic those in functional assay. In this case,  $K_A$  should be determined at

	pEC <sub>50</sub>	E' <sub>MAX</sub>	pK <sub>A</sub>	τ
<b>[<sup>35</sup>S]GTPγS binding, E<sub>MAX</sub> = 7.33</b>				
Arecoline	6.94 ± 0.03	3.8 ± 0.2	6.6 ± 0.1	1.09 ± 0.08
Carbachol	6.77 ± 0.03	3.7 ± 0.2	6.5 ± 0.1	1.06 ± 0.08
Furmethide	6.48 ± 0.03	3.9 ± 0.2	6.1 ± 0.1	1.17 ± 0.09
Iperoxo	8.09 ± 0.02	5.9 ± 0.3	7.4 ± 0.1	4.3 ± 0.4
McN-A-343	6.70 ± 0.03	3.3 ± 0.2	6.4 ± 0.1	0.80 ± 0.06
NDMC	6.84 ± 0.03	3.2 ± 0.2	6.6 ± 0.1	0.79 ± 0.06
Oxotremorine	7.73 ± 0.02	4.7 ± 0.3	7.3 ± 0.1	1.75 ± 0.14
Pilocarpine	6.80 ± 0.03	2.6 ± 0.1	6.6 ± 0.1	0.54 ± 0.04
Xanomeline	8.34 ± 0.02	4.1 ± 0.2	8.0 ± 0.1	1.24 ± 0.10
<b>IP<sub>x</sub> level, E<sub>MAX</sub> = 5.75</b>				
Arecoline	7.02 ± 0.02	3.6 ± 0.2	6.6 ± 0.1	1.67 ± 0.15
Carbachol	6.87 ± 0.03	3.5 ± 0.2	6.5 ± 0.1	1.50 ± 0.13
Furmethide	6.57 ± 0.03	3.7 ± 0.2	6.1 ± 0.1	1.78 ± 0.16
Iperoxo	8.23 ± 0.02	5.0 ± 0.3	7.4 ± 0.1	6.7 ± 0.7
McN-A-343	6.77 ± 0.03	3.2 ± 0.2	6.4 ± 0.1	1.21 ± 0.09
NDMC	6.88 ± 0.03	3.1 ± 0.2	6.5 ± 0.1	1.19 ± 0.08
Oxotremorine	7.84 ± 0.02	4.2 ± 0.2	7.3 ± 0.1	2.59 ± 0.21
Pilocarpine	6.85 ± 0.02	2.5 ± 0.1	6.6 ± 0.1	0.78 ± 0.06
Xanomeline	8.46 ± 0.02	3.7 ± 0.2	8.0 ± 0.1	1.83 ± 0.15
<b>Intracellular Ca<sup>2+</sup> level, E<sub>MAX</sub> = 1.879</b>				
Arecoline	8.19 ± 0.02	1.828 ± 0.003	6.6 ± 0.1	35 ± 5
Carbachol	7.96 ± 0.03	1.829 ± 0.003	6.4 ± 0.1	33 ± 5
Furmethide	7.73 ± 0.03	1.830 ± 0.003	6.1 ± 0.1	38 ± 6
Iperoxo	9.53 ± 0.02	1.839 ± 0.003	7.3 ± 0.1	156 ± 51
McN-A-343	7.85 ± 0.03	1.820 ± 0.003	6.4 ± 0.1	27 ± 5
NDMC	8.01 ± 0.03	1.816 ± 0.003	6.6 ± 0.1	26 ± 4
Oxotremorine	9.07 ± 0.02	1.831 ± 0.003	7.3 ± 0.1	64 ± 14
Pilocarpine	7.85 ± 0.02	1.791 ± 0.003	6.6 ± 0.1	18 ± 3
Xanomeline	9.65 ± 0.02	1.834 ± 0.003	8.0 ± 0.1	44 ± 8

**Table 7.** Parameters of functional response of M<sub>2</sub>-G<sub>15</sub> fusion protein to muscarinic agonists. Eq. (10) was fitted to individual data sets. Eq. (6) was fitted to E'<sub>MAX</sub> versus EC<sub>50</sub> data from all 3 experiments for all agonists to obtain E<sub>MAX</sub> of the assay. Equation (1) with fixed E<sub>MAX</sub> was fitted to individual functional responses. Data are means ± SD from 3 independent experiments.

whole cells attached to the bottom of 96-well plate. In whole cells, agonists display low-affinity binding that is the result of negative cooperativity between binding of GDP and binding of an agonist to the receptor G-protein complex<sup>20</sup>. K<sub>A</sub> is the ratio between the experimentally calculated low-affinity K<sub>i</sub> and factor of binding cooperativity of GDP and agonist. As far as the factor of binding cooperativity is unknown, K<sub>A</sub> cannot be calculated. In membranes, muscarinic agonists usually display both high- and low-affinity binding<sup>21</sup> as free GDP is removed and bound GDP partly dissociates during membrane preparation. At the M<sub>2</sub>-G<sub>15</sub> and M<sub>4</sub>-G<sub>15</sub> fusion proteins, however, inhibition of [<sup>3</sup>H]NMS binding by tested agonists showed only low-affinity binding (Table 4). It is possible that at constructed fusion proteins interaction of G-protein with the receptor in an inactive conformation is very strong and that GDP is locked in its binding site at G-protein<sup>22</sup>. The locking precludes dissociation of GDP from the G-protein. An open question remains, namely whether K<sub>i</sub> of agonist high-affinity binding observed in membranes can be taken as K<sub>A</sub>. Actually, K<sub>A</sub> may be affected by many factors including binding cooperativity between agonist and GDP-less G-protein and by changes resulting from membrane preparation. Taking this into account, it may be actually safer to determine K<sub>A</sub> from a series of functional experiments according to the procedure described below than to determine K<sub>A</sub> in radioligand binding assays.

Indeed, inhibition constants K<sub>i</sub> of low-affinity agonist binding were too high to be considered as K<sub>A</sub>. Considering that K<sub>A</sub> equals K<sub>i</sub> (Supplementary Information, Figs SI3–SI8) resulted in high values of τ as a result of high K<sub>A</sub> to EC<sub>50</sub> ratio (Eq. d). For high values of τ apparent maximal response E'<sub>MAX</sub> approximates maximal response of the system E<sub>MAX</sub> (Eq. (3)). Thus variation in E<sub>MAX</sub> caused variation in E'<sub>MAX</sub>. However, E<sub>MAX</sub> should be the same for all 5 cell clones. Global fit of Eq. (1) to functional response data in all 5 cell clones with shared E'<sub>MAX</sub> did not converge (Supplementary Information, Figs SI3–SI8, yellow dotted lines).

Therefore, a novel procedure to obtain reliable values of K<sub>A</sub> and E<sub>MAX</sub> by meta-analysis of functional response data was developed. Analysis of the OM according to Eq. (1) shows that the apparent maximal response E'<sub>MAX</sub> relates to the maximal response of the system E<sub>MAX</sub> according to Eq. (3) and EC<sub>50</sub> relates to K<sub>A</sub> according to Eq. (4). E'<sub>MAX</sub> and EC<sub>50</sub> were obtained by fitting Eq. (10) to data of individual functional responses (Figs 2 and 3, left and right upper and left lower plots, full lines). Subsequently, E'<sub>MAX</sub> values were taken as a function of

	pEC <sub>50</sub>	E' <sub>MAX</sub>	pK <sub>A</sub>	τ
<b>[<sup>35</sup>S]GTPγS binding, E<sub>MAX</sub> = 6.85</b>				
Arecoline	6.98 ± 0.03	4.2 ± 0.2	6.6 ± 0.1	1.60 ± 0.12
Carbachol	6.94 ± 0.03	4.3 ± 0.2	6.5 ± 0.1	1.74 ± 0.13
Furmethide	6.58 ± 0.03	4.4 ± 0.2	6.1 ± 0.1	1.77 ± 0.13
Iperoxo	7.88 ± 0.02	5.0 ± 0.3	7.3 ± 0.1	2.70 ± 0.22
McN-A-343	6.86 ± 0.03	4.0 ± 0.2	6.5 ± 0.1	1.43 ± 0.12
NDMC	7.01 ± 0.03	3.9 ± 0.2	6.6 ± 0.1	1.32 ± 0.11
Oxotremorine	7.77 ± 0.02	4.4 ± 0.2	7.3 ± 0.1	1.84 ± 0.13
Pilocarpine	6.78 ± 0.03	3.0 ± 0.2	6.5 ± 0.1	0.80 ± 0.06
Xanomeline	8.50 ± 0.02	4.6 ± 0.2	8.0 ± 0.1	2.06 ± 0.16
<b>IP<sub>x</sub> level, E<sub>MAX</sub> = 4.18</b>				
Arecoline	7.10 ± 0.02	2.9 ± 0.1	6.6 ± 0.1	2.37 ± 0.22
Carbachol	7.02 ± 0.03	3.0 ± 0.2	6.5 ± 0.1	2.45 ± 0.23
Furmethide	6.67 ± 0.03	3.0 ± 0.2	6.1 ± 0.1	2.57 ± 0.25
Iperoxo	7.97 ± 0.02	3.3 ± 0.2	7.3 ± 0.1	3.9 ± 0.4
McN-A-343	6.92 ± 0.03	2.8 ± 0.1	6.5 ± 0.1	1.96 ± 0.18
NDMC	7.10 ± 0.03	2.7 ± 0.1	6.7 ± 0.1	1.79 ± 0.16
Oxotremorine	7.82 ± 0.02	3.0 ± 0.2	7.3 ± 0.1	2.48 ± 0.24
Pilocarpine	6.85 ± 0.02	2.2 ± 0.1	6.5 ± 0.1	1.08 ± 0.09
Xanomeline	8.62 ± 0.02	3.1 ± 0.2	8.0 ± 0.1	2.77 ± 0.28
<b>Intracellular Ca<sup>2+</sup> level, E<sub>MAX</sub> = 1.861</b>				
Arecoline	8.32 ± 0.02	1.828 ± 0.003	6.6 ± 0.1	57 ± 10
Carbachol	8.22 ± 0.03	1.829 ± 0.003	6.4 ± 0.1	59 ± 10
Furmethide	7.93 ± 0.03	1.830 ± 0.003	6.1 ± 0.1	61 ± 11
Iperoxo	9.27 ± 0.02	1.839 ± 0.003	7.3 ± 0.1	87 ± 29
McN-A-343	8.08 ± 0.03	1.820 ± 0.003	6.4 ± 0.1	45 ± 5
NDMC	8.24 ± 0.03	1.816 ± 0.003	6.6 ± 0.1	41 ± 6
Oxotremorine	9.05 ± 0.02	1.831 ± 0.003	7.2 ± 0.1	63 ± 11
Pilocarpine	8.00 ± 0.02	1.791 ± 0.003	6.6 ± 0.1	26 ± 4
Xanomeline	9.93 ± 0.02	1.834 ± 0.003	8.1 ± 0.1	71 ± 14

**Table 8.** Parameters of functional response of M<sub>4</sub>G<sub>15</sub> fusion protein to muscarinic agonists. Equation (10) was fitted to individual data sets. Equation (6) was fitted to E'<sub>MAX</sub> versus EC<sub>50</sub> data from all 3 experiments for all agonists to obtain E<sub>MAX</sub> of the assay. Equation (1) with fixed E<sub>MAX</sub> was fitted to individual functional responses. Data are means ± SD from 3 independent experiments.

corresponding EC<sub>50</sub> values and parameters E<sub>MAX</sub> and K<sub>A</sub> were obtained by fitting Eq. (6) (Figs 2 and 3, right lower plot). Obtained E<sub>MAX</sub> and K<sub>A</sub> values (Tables 5 and 6) were used to globally fit Eq. (1) to functional response data (Figs 2 and 3, left and right upper and left lower plots, dotted yellow lines). With only one exception SD of τ estimates was well below 10% (Tables 5 and 6). That is a great improvement over direct fitting of Eq. (1) to the functional data (Supplementary Information, Figs SI3–SI8).

Another possibility how to reduce the number of degrees of freedom in the fitting of the OM to data is to fix E<sub>MAX</sub>. In case of accumulation of inositol phosphates, it may seem intuitive that 100% of incorporated radioactivity may be metabolized to inositol trisphosphate, and that is the actual maximal response of the system (E<sub>MAX</sub>). However, as shown by presented experimental data E<sub>MAX</sub> is around 90% of incorporated radioactivity. This is given by the fact that converting substrate to product decreases substrate level and increases product level, resulting in feedback inhibition of the forward reaction. The level at which the reaction comes to equilibrium between substrate and product may be affected by various other factors (e.g. starting concentration of substrate, inhibition of subsequent metabolic steps, related metabolic processes). In case of [<sup>35</sup>S]GTPγS binding, the amount of GTPγS is greater than the amount of G-protein. Therefore, it may seem intuitive that 100% occupancy of G-protein represents the E<sub>MAX</sub>. However, E<sub>MAX</sub> expressed as occupancy of G-protein in this assay is less than 20%. In case of intracellular calcium, E<sub>MAX</sub> is given by the ratio of the rate of calcium release from intracellular stores to the rate of calcium clearance from cytoplasm. Thus, E<sub>MAX</sub> cannot be established *a priori* and needs to be measured experimentally. Fitting Eq. (6) to E'<sub>MAX</sub> versus EC<sub>50</sub> data allows calculation of the E<sub>MAX</sub> of the assay.

A drawback of the described procedure is that at least 3 systems (cell clones) with substantially different receptor expression level are needed to fit Eq. (6) to functional response meta-data for a given agonist. Having only 2 systems can be overcome by combining 3 or more agonists substantially differing in efficacy for a global fit of Eq. (6) to functional response meta-data (Figs 2 and 3, lower right plot, green dotted lines). Having only one system (Figs 4 and 5, Tables 7 and 8), the first step for ranking a batch of agonists in terms of efficacy is to fit Eq. (10) to individual functional responses. After subtraction of basal value the relationship between E'<sub>MAX</sub> and EC<sub>50</sub> for all agonists was fitted to Eq. (6) to obtain E<sub>MAX</sub> of the assay. Finally, one fits Eq. (1) with fixed E<sub>MAX</sub> to individual functional responses.

Regardless the number of systems employed, the procedure is limited to conditions with substantially different  $\tau$  values ranging from 0.1 to 100. The procedure will not work when only agonists with  $\tau$  greater than 100 are available as  $K_A$  could not be properly estimated using Eq. (6). Such situation should be resolved experimentally by reduction of receptor number using an irreversible antagonist that will bring  $\tau$  values down to allow  $K_A$  determination. Similarly, if only very weak agonists with  $\tau$  lower than 0.1 are available, then the procedure will not work either as system  $E_{MAX}$  could not be properly estimated using Eq. (6). In such case, a highly efficacious agonist needs to be added for comparison. Measurements of intracellular  $Ca^{2+}$  (Figs 4 and 5, Tables 7 and 8) show that our procedure can be used in a system where  $E'_{MAX}$  of agonists approaches  $E_{MAX}$  of the system; a case where direct fitting of OM would be problematic.

In principle, the procedure described above can be used everywhere OM is applicable including other G-protein coupled receptors or any receptor-effector system in general<sup>1,2</sup>. Moreover, the procedure can also be applied to all possible variants of the OM as far as relations between parameters of the OM variant and parameters of classical (e.g. logistic) function can be established. For example, introducing the slope factor (Hill coefficient) to Eq. (1) does not change the relation of  $EC_{50}$  to  $K_A$  and  $E'_{MAX}$  to  $E_{MAX}$  as slope factor cancels out itself in Eqs (2) and (3).

## Conclusions

Described two-step analysis of functional response represents the robust way of fitting operational model of agonism (OM) to experimental data. Although our procedure was developed using muscarinic acetylcholine receptors as a test system, it is in principle applicable to any receptor-effector system where OM is used. Also, the procedure can be applied to all possible variants of the OM as far as relations between parameters of the OM variant and parameters of classical (e.g. logistic) function can be established. We believe the procedure will have significant practical value in the proper ranking of agonists efficacies in various systems.

## Methods

**Receptor mutagenesis and generation of cell lines.** New stable Chinese hamster ovary (CHO) cells lines expressing fusion proteins of  $M_2$  or  $M_4$  receptors and  $G_{15}$  G-protein were prepared. Plasmid pcDNA3.1 (Invitrogen) containing the coding sequence of the human variants of muscarinic receptors and that of the  $G_{15}$  G-protein were obtained from Missouri S&T cDNA Resource Center (Rolla, MO, USA). Mammalian vector with hygromycin as mammalian selection marker pCMV6-A-Hygro was purchased from Origene (Rockville, MD). First, the  $G_{15}$  G-protein coding sequence was subcloned into pCMV6-A-Hygro plasmid. Then AflII sites were generated at the 3'-end of coding sequence of  $M_2$  and  $M_4$  using Quick Change II Site-directed Mutagenesis Kit (Stratagene). The coding sequence of the receptor was subcloned into  $G_{15}$ -pCMV-A-Hygro plasmid. The  $M_2$  coding sequence was ligated directly to the  $G_{15}$  coding sequence. In case of the  $M_4$  receptor, ARATR linker was inserted between the receptor and the G-protein (resulting sequences are in Supplementary Information). CHO-K1 cells were transfected with the desired plasmids using Lipofectamine 3000 (Invitrogen). Subconfluent cells were washed with phosphate-buffered saline and then Opti-MEM (Life Technologies) containing Lipofectamine at a final concentration of 1.5  $\mu$ l/ml and plasmid DNA was applied at a final concentration of 0.5  $\mu$ g/ml. After 48 hours cells were diluted 1000-times by subculturing and hygromycin-B (Toku-E) was added at final concentration of 200 ng/ml for selection of transfected clones. For the study 5 clones of each construct selected from the single selection were used up to passage 10. Expression of new constructs was checked by reverse transcription quantitative PCR. Mediator RNA was isolated from CHO cell lines using TriPure Isolation Reagent (Roche). Reverse transcription was done using M-MLV Reverse Transcriptase (Promega), Oligo (dT) anchored primers and quantified using LightCycler<sup>®</sup> 480 SYBR Green I Master in LightCycler<sup>®</sup> 480 Instrument II system (Roche) and analyzed by LightCycler<sup>®</sup> 480 Software 1.5.0.

**Cell culture and membrane preparation.** CHO cells were grown to confluence in 75 cm<sup>2</sup> flasks in Dulbecco's modified Eagle's medium (DMEM) supplemented with 10% fetal bovine serum. Two million cells were subcultured in 100-mm Petri dishes. The medium was supplemented with 5 mM sodium butyrate for the last 24 hours of cultivation to increase receptor expression. Cells were washed with phosphate-buffered saline and manually harvested on day 5 after subculture and centrifuged for 3 min at 250  $\times$  g. The pellet was suspended in 10 ml of ice-cold homogenization medium (100 mM NaCl, 20 mM Na-HEPES, 10 mM EDTA, pH = 7.4) and homogenized on ice by two 30 sec strokes using a Polytron homogenizer (Ultra-Turrax; Janke & Kunkel GmbH & Co. KG, IKA-Labortechnik, Staufen, Germany) with a 30-sec pause between strokes. Cell homogenates were centrifuged for 5 min at 1000  $\times$  g. The supernatant was collected and centrifuged for 30 min at 30,000  $\times$  g. Pellets were suspended in the washing medium (100 mM, 10 mM MgCl<sub>2</sub>, 20 mM Na-HEPES, pH = 7.4), left for 30 min at 4  $^{\circ}$ C, and then centrifuged again for 30 min at 30,000  $\times$  g. Resulting membrane pellets were kept at  $-80^{\circ}$ C until assayed.

**Radioligand binding experiments.** All radioligand binding experiments were optimized and carried out according to general guidelines<sup>23</sup>. Membranes (5 to 10  $\mu$ g of membrane proteins per sample for [<sup>35</sup>S]GTP $\gamma$ S binding or 20 to 50  $\mu$ g of membrane proteins per sample for [<sup>3</sup>H]NMS binding) were used. Agonist binding was determined in competition experiments with 1 nM [<sup>3</sup>H]NMS. Membranes were incubated for 3 hours at 37  $^{\circ}$ C in 400  $\mu$ l of Krebs-HEPES buffer (KHB; final concentrations in mM: NaCl 138; KCl 4; CaCl<sub>2</sub> 1.3; MgCl<sub>2</sub> 1; NaH<sub>2</sub>PO<sub>4</sub> 1.2; HEPES 20; glucose 10; pH adjusted to 7.4). In saturation experiments of binding of [<sup>3</sup>H]N-methylscopolamine ([<sup>3</sup>H]NMS) six concentrations of the radioligand (ranging from 63 to 2000 pM) were used and incubation volume was increased to 0.8 ml. Nonspecific binding was determined in the presence of 10  $\mu$ M atropine.

Agonist-stimulated [<sup>35</sup>S]GTPγS binding was measured in a final volume of 200 μl of washing medium with 500 pM [<sup>35</sup>S]GTPγS and 50 μM GDP for 20 min at 30 °C after 60 min preincubation with GDP and agonist. Nonspecific binding was determined in the presence of 1 μM unlabeled GTPγS.

Incubation was terminated by filtration through Whatman GF/C glass fiber filters (Whatman) using a Brandel harvester (Brandel, USA). Filters were dried in a microwave oven (3 min, 800 W) and then solid scintillator Meltilex A was melted on filters (90 °C, 70 s) using a hot plate. The filters were cooled and counted in a Wallac Microbeta scintillation counter (Wallac, Finland).

**Accumulation of inositol phosphates.** Accumulation of inositol phosphates (IP<sub>x</sub>) was assayed in cells grown in 96-well plates. The cells were loaded with 200 nM [<sup>3</sup>H]myo-inositol (ARC, USA) in DMEM overnight. Then DMEM was removed and the cells were washed with 100 μl KHB. Then cells were incubated with agonists at 200 μl of KHB containing 10 mM LiCl for 1 hour at 37 °C. Incubation was terminated by the removal of incubation medium and addition of 50 μl of 20% trichloroacetic acid (TCA). Plates were kept at 4 °C for 1 hour, then 40 μl of TCA extract were transferred to another 96-well plate, mixed with 200 μl of Rotiszint scintillation cocktail and counted in Wallac Microbeta. Rest of TCA extract was discarded, individual wells were washed with 50 μl of 20% TCA, 50 μl of 1 M NaOH was added to each well and plates were shaken at room temperature for 15 min. Then 40 μl of NaOH lysate were transferred to another 96-well plate, mixed with 200 μl of Rotiszint scintillation cocktail (Carl Roth, Germany) and counted in Wallac Microbeta. Level of inositol phosphates was calculated as a fraction of soluble (TCA extract) to total (TCA extract plus NaOH lysate) radioactivity.

**Microfluorometry of free intracellular calcium.** Cells grown on glass coverslips were washed twice with KHB and then prelabelled with 5 μM Fura 2-AM in KHB enriched with 1 mM pluronic P68 for one hour at 37 °C. After prelabelling cells were washed twice with KHB, mounted to a superfusion chamber, placed on a stage of Olympus IX-90 inverted fluorescent microscope, and continuously superfused at a flow rate 0.5 ml/min. Microfluorometry was set-up to measure kinetics of the functional response to agonists. Cells expressing fusion proteins of muscarinic receptors and G<sub>15</sub> G-protein were exposed to 5 increasing concentrations of agonist for 10 s. Individual exposures were separated by 10 min superfusion with agonist-free KHB medium. Images were recorded using a CCD camera connected to a computer equipped with Metafluor 7.0 software (Visitron Systems GmBH, Germany) for image acquisition and analysis. Images of the whole measured field containing about 40 cells were saved and analysed off-line after the measurements. Two pairs of images per second were recorded. Only responding cells were selected (by exclusion of weakly and/or slow responding cells or cells with abnormal response; the outliers in peak value, time to peak or fall time were identified by interquartile range (IQR) where data below Q1-1.5\*IQR and above Q3 + 1.5\*IQR were considered outliers) for further analysis. Calcium signals of selected cells were averaged, normalized to basal calcium level and further analysed by means of array-oriented program Grace (<http://plasma-gate.weizmann.ac.il/Grace>).

**Generation and analysis of theoretical data.** Whole processes of the theoretical data generation, non-linear regression and analysis of the results were automated by scripts written in Python 2.7. Theoretical data with 3% of proportional noise were simulated by NumPy package. Non-linear regression was performed using optimize function of SciPy package. Standard deviations of estimated parameters were calculated from Jacobian covariance matrix. For control the standard deviations were computed by bootstrap method. Data and fits were visualized by Matplotlib package.

**Analysis of experimental data.** Data from experiments were processed in Libre Office and then analyzed and plotted using program Grace (<http://plasma-gate.weizmann.ac.il/Grace>). Statistical analysis was performed using statistical package R (<http://www.R-project.org>). The following equations were used for non-linear regression analysis:

[<sup>3</sup>H]NMS saturation binding.

$$y = \frac{B_{\text{MAX}} * x}{x + K_D} \quad (7)$$

where y is specific binding at free concentration x, B<sub>MAX</sub> is the maximum binding capacity, and K<sub>D</sub> is the equilibrium dissociation constant.

Competition binding.

$$y = 100 - \frac{(100 - f_{\text{low}}) * x}{x + IC_{50\text{high}}} - \frac{f_{\text{low}} * x}{x + IC_{50\text{low}}} \quad (8)$$

where y is specific radioligand binding at concentration x of competitor expressed as per cent of binding in the absence of competitor, IC<sub>50</sub> is the concentration causing 50% inhibition of radioligand binding at high (IC<sub>50high</sub>) and low (IC<sub>50low</sub>) affinity binding sites, f<sub>low</sub> is the fraction of low affinity binding sites expressed in per cent. Inhibition constant K<sub>I</sub> was calculated as:

$$K_I = \frac{IC_{50}}{1 + \frac{[D]}{K_D}} \quad (9)$$

where [D] is the concentration of radioligand used and K<sub>D</sub> is its equilibrium dissociation constant.

Concentration response curve.

$$y = 1 + \frac{(E'_{MAX} - 1) * x^{nH}}{x^{nH} + EC_{50}^{nH}} \quad (10)$$

where  $y$  is response normalized to basal activity at concentration  $x$ ,  $E'_{MAX}$  is apparent maximal response,  $EC_{50}$  is concentration causing half-maximal effect, and  $nH$  is Hill coefficient.

## References

- Black, J. W. & Leff, P. Operational models of pharmacological agonism. *Proc. R. Soc. London. Ser. B, Biol. Sci.* **220**, 141–62 (1983).
- Leff, P., Dougall, I. G. & Harper, D. Estimation of partial agonist affinity by interaction with a full agonist: a direct operational model fitting approach. *Br. J. Pharmacol.* **110**, 239–244 (1993).
- Kenakin, T. Efficacy as a Vector: the Relative Prevalence and Paucity of Inverse Agonism. *Mol. Pharmacol.* **65**, 2–11 (2004).
- Kenakin, T. New concepts in pharmacological efficacy at 7TM receptors: IUPHAR Review 2. *Br. J. Pharmacol.* **168**, 554–575 (2013).
- Kenakin, T. Agonist-receptor efficacy I: mechanisms of efficacy and receptor promiscuity. *Trends Pharmacol. Sci.* **16**, 188–192 (1995).
- Frigyesi, A. & Hössjer, O. Estimating the parameters of the operational model of pharmacological agonism. *Stat. Med.* **25**, 2932–2945 (2006).
- Christopoulos, A. Assessing the distribution of parameters in models of ligand-receptor interaction: To log or not to log. *Trends Pharmacol. Sci.* **19**, 351–357 (1998).
- Boulos, J. F., Jakubik, J., Boulos, J. M., Randakova, A. & Momirov, J. Synthesis of novel and functionally selective non-competitive muscarinic antagonists as chemical probes. *Chem. Biol. Drug Des.* **91**, 93–104 (2018).
- Offermanns, S. & Simon, M. I. G alpha 15 and G alpha 16 couple a wide variety of receptors to phospholipase C. *J Biol Chem* **270**, 15175–15180 (1995).
- Ehlert, F. J. Analysis of allosterism in functional assays. *J.Pharmacol.Exp.Ther.* **315**, 740–754 (2005).
- Sawyer, G. W., Ehlert, F. J. & Shults, C. A. Cysteine pairs in the third intracellular loop of the muscarinic m1 acetylcholine receptor play a role in agonist-induced internalization. *J Pharmacol Exp Ther* **324**, 196–205 (2008).
- Smith, N. J. *et al.* Extracellular Loop 2 of the Free Fatty Acid Receptor 2 Mediates Allosterism of a Phenylacetamide Ago-Allosteric Modulator. *Molecular Pharmacol.* **80**, 163–173 (2011).
- Abdul-Ridha, A. *et al.* Mechanistic Insights into Allosteric Structure-Function Relationships at the M<sub>1</sub> Muscarinic Acetylcholine Receptor. *J. Biol. Chem.* **289**, 33701–33711 (2014).
- Abdul-Ridha, A. *et al.* Molecular Determinants of Allosteric Modulation at the M<sub>1</sub> Muscarinic Acetylcholine Receptor. *J. Biol. Chem.* **289**, 6067–6079 (2014).
- Kenakin, T. & Christopoulos, A. Signalling bias in new drug discovery: detection, quantification and therapeutic impact. *Nat Rev Drug Discov* **12**, 205–216 (2013).
- van der Westhuizen, E. T., Breton, B., Christopoulos, A. & Bouvier, M. Quantification of Ligand Bias for Clinically Relevant 2-Adrenergic Receptor Ligands: Implications for Drug Taxonomy. *Mol. Pharmacol.* **85**, 492–509 (2014).
- Thompson, G. L. *et al.* Systematic analysis of factors influencing observations of biased agonism at the mu-opioid receptor. *Biochem. Pharmacol.* **113**, 70–87 (2016).
- Kenakin, T. Theoretical aspects of GPCR-ligand complex pharmacology. *Chem. Rev.* **117**, 4–20 (2017).
- Bedinger, D. H., Goldfine, I. D., Corbin, J. A., Roell, M. K. & Adams, S. H. Differential pathway coupling of the activated insulin receptor drives signaling selectivity by XMetA, an allosteric partial agonist antibody. *J. Pharmacol. Exp. Ther.* **353**, 35–43 (2015).
- Jakubik, J., Janičková, H., El-Fakahany, E. E. & Doležal, V. Negative cooperativity in binding of muscarinic receptor agonists and GDP as a measure of agonist efficacy. *Br J Pharmacol* **162**, 1029–1044 (2011).
- Waelbroeck, M., Robberecht, P., Chatelain, P. & Christophe, J. Rat cardiac muscarinic receptors. I. Effects of guanine nucleotides on high- and low-affinity binding sites. *Mol. Pharmacol.* **21**, 581 LP–588 (1982).
- DeVree, B. T. *et al.* Allosteric coupling from G protein to the agonist-binding pocket in GPCRs. *Nature* **535**, 182–6 (2016).
- El-Fakahany, E. E. & Jakubik, J. In *Muscarinic Receptor: From Structure to Animal Models* (eds Myslivecek, J. & Jakubik, J.) 37–68, [https://doi.org/10.1007/978-1-4939-2858-3\\_3](https://doi.org/10.1007/978-1-4939-2858-3_3) (Springer New York, 2016).

## Acknowledgements

This work was supported by the Czech Academy of Sciences [RVO:67985823] and the Grant Agency of the Czech Republic [17–16182 S].

## Author Contributions

J.J. conducted the analysis of fitting of the operational model to simulated data. P.Z. and A.R. prepared cDNA of fusion proteins and stable CHO cell lines. A.R. and V.R. measured binding of and functional response to agonists. A.R. and J.J. analysed the data. J.J. supervised this study. J.J., E.E.E. and V.D. wrote the manuscript. All authors read and approved the final manuscript.

## Additional Information

**Supplementary information** accompanies this paper at <https://doi.org/10.1038/s41598-019-40993-w>.

**Competing Interests:** The authors declare that the authors have no competing interests as defined by Nature Research, or other interests that might be perceived to influence the results and/or discussion reported in this paper.

**Publisher's note:** Springer Nature remains neutral with regard to jurisdictional claims in published maps and institutional affiliations.



**Open Access** This article is licensed under a Creative Commons Attribution 4.0 International License, which permits use, sharing, adaptation, distribution and reproduction in any medium or format, as long as you give appropriate credit to the original author(s) and the source, provide a link to the Creative Commons license, and indicate if changes were made. The images or other third party material in this article are included in the article's Creative Commons license, unless indicated otherwise in a credit line to the material. If material is not included in the article's Creative Commons license and your intended use is not permitted by statutory regulation or exceeds the permitted use, you will need to obtain permission directly from the copyright holder. To view a copy of this license, visit <http://creativecommons.org/licenses/by/4.0/>.

© The Author(s) 2019